

# Transverse target single-spin asymmetry in inclusive electroproduction of charged pions and kaons

A. Airapetian<sup>m,p</sup>, N. Akopov<sup>aa</sup>, Z. Akopov<sup>f</sup>, E.C. Aschenauer<sup>g,1</sup>, W. Augustyniak<sup>z</sup>, R. Avakian<sup>aa</sup>, A. Avetissian<sup>aa</sup>, E. Avetisyan<sup>f</sup>, S. Belostotski<sup>s</sup>, N. Bianchi<sup>k</sup>, H.P. Blok<sup>t,y</sup>, A. Borissov<sup>l</sup>, J. Bowles<sup>n</sup>, V. Bryzgalov<sup>l</sup>, J. Burns<sup>n</sup>, M. Capiluppi<sup>j</sup>, G.P. Capitani<sup>k</sup>, E. Cisbani<sup>v</sup>, G. Ciullo<sup>j</sup>, M. Contalbrigo<sup>j</sup>, P.F. Dalpiaz<sup>j</sup>, W. Deconinck<sup>f</sup>, R. De Leo<sup>b</sup>, L. De Nardo<sup>l,f,w</sup>, E. De Sanctis<sup>k</sup>, M. Diefenthaler<sup>o,i</sup>, P. Di Nezza<sup>k</sup>, M. Düren<sup>m</sup>, M. Ehrenfried<sup>m</sup>, G. Elbakian<sup>aa</sup>, F. Ellinghaus<sup>e</sup>, R. Fabbri<sup>g</sup>, A. Fantoni<sup>k</sup>, L. Felawka<sup>w</sup>, S. Frullani<sup>v</sup>, D. Gabbert<sup>g</sup>, G. Gapienko<sup>l</sup>, V. Gapienko<sup>l</sup>, G. Gavrilo<sup>f,s,w</sup>, V. Gharibyan<sup>aa</sup>, F. Giordano<sup>o,j</sup>, S. Gliske<sup>p</sup>, M. Golembiovskaya<sup>g</sup>, C. Hadjidakis<sup>k</sup>, M. Hartig<sup>f</sup>, D. Hasch<sup>k</sup>, A. Hillenbrand<sup>g</sup>, M. Hoek<sup>n</sup>, Y. Holler<sup>f</sup>, I. Hristova<sup>g</sup>, A. Ivanilov<sup>l</sup>, H.E. Jackson<sup>a</sup>, S. Joosten<sup>o,l</sup>, R. Kaiser<sup>n</sup>, G. Karyan<sup>aa</sup>, T. Keri<sup>n,m</sup>, E. Kinney<sup>e</sup>, A. Kisselev<sup>s</sup>, V. Korotkov<sup>l</sup>, V. Kozlov<sup>q</sup>, P. Kravchenko<sup>i,s</sup>, V.G. Krivokhijine<sup>h</sup>, L. Lagamba<sup>b</sup>, L. Lapikás<sup>r</sup>, I. Lehmann<sup>n</sup>, P. Lenisa<sup>j</sup>, A. López Ruiz<sup>l</sup>, W. Lorenzon<sup>p</sup>, B.-Q. Ma<sup>c</sup>, D. Mahon<sup>n</sup>, N.C.R. Makins<sup>o</sup>, S.I. Manaenkov<sup>s</sup>, Y. Mao<sup>c</sup>, B. Marianski<sup>z</sup>, A. Martínez de la Ossa<sup>f,e</sup>, H. Marukyan<sup>aa</sup>, C.A. Miller<sup>w</sup>, Y. Miyachi<sup>x</sup>, A. Movsisyan<sup>i,aa</sup>, M. Murray<sup>n</sup>, A. Mussgiller<sup>f,i</sup>, E. Nappi<sup>b</sup>, Y. Naryshkin<sup>s</sup>, M. Negodaev<sup>g</sup>, W.-D. Nowak<sup>g</sup>, L.L. Pappalardo<sup>j</sup>, R. Perez-Benito<sup>m</sup>, A. Petrosyan<sup>aa</sup>, M. Raithel<sup>i</sup>, P.E. Reimer<sup>a</sup>, A.R. Reolon<sup>k</sup>, C. Riedl<sup>o,g</sup>, K. Rith<sup>i</sup>, G. Rosner<sup>n</sup>, A. Rostomyan<sup>f</sup>, J. Rubin<sup>a,o</sup>, D. Ryckbosch<sup>l</sup>, Y. Salomatin<sup>l</sup>, F. Sanftl<sup>x,u</sup>, A. Schäfer<sup>r</sup>, G. Schnell<sup>d,l</sup>, B. Seitz<sup>n</sup>, T.-A. Shibata<sup>x</sup>, V. Shutov<sup>h</sup>, M. Stancari<sup>j</sup>, M. Statera<sup>j</sup>, E. Steffens<sup>i</sup>, J.J.M. Steijger<sup>r</sup>, J. Stewart<sup>g</sup>, F. Stinzinger<sup>i</sup>, S. Taroian<sup>aa</sup>, A. Terkulov<sup>q</sup>, R. Truty<sup>o</sup>, A. Trzcinski<sup>z</sup>, M. Tytgat<sup>l</sup>, Y. Van Haarlem<sup>l</sup>, C. Van Hulse<sup>d,l</sup>, D. Veretennikov<sup>s</sup>, V. Vikhrov<sup>s</sup>, I. Vilardi<sup>b</sup>, S. Wang<sup>c</sup>, S. Yaschenko<sup>g,i</sup>, Z. Ye<sup>f</sup>, S. Yen<sup>w</sup>, W. Yu<sup>m</sup>, V. Zagrebelny<sup>f,m</sup>, D. Zeiler<sup>i</sup>, B. Zihlmann<sup>f</sup>, P. Zupranski<sup>z</sup>,

(The HERMES Collaboration)

<sup>a</sup>Physics Division, Argonne National Laboratory, Argonne, Illinois 60439-4843, USA

<sup>b</sup>Istituto Nazionale di Fisica Nucleare, Sezione di Bari, 70124 Bari, Italy

<sup>c</sup>School of Physics, Peking University, Beijing 100871, China

<sup>d</sup>Department of Theoretical Physics, University of the Basque Country UPV/EHU, 48080 Bilbao, Spain and IKERBASQUE, Basque Foundation for Science, 48011 Bilbao, Spain

<sup>e</sup>Nuclear Physics Laboratory, University of Colorado, Boulder, Colorado 80309-0390, USA

<sup>f</sup>DESY, 22603 Hamburg, Germany

<sup>g</sup>DESY, 15738 Zeuthen, Germany

<sup>h</sup>Joint Institute for Nuclear Research, 141980 Dubna, Russia

<sup>i</sup>Physikalisches Institut, Universität Erlangen-Nürnberg, 91058 Erlangen, Germany

<sup>j</sup>Istituto Nazionale di Fisica Nucleare, Sezione di Ferrara and Dipartimento di Fisica e Scienze della Terra, Università di Ferrara, 44122 Ferrara, Italy

<sup>k</sup>Istituto Nazionale di Fisica Nucleare, Laboratori Nazionali di Frascati, 00044 Frascati, Italy

<sup>l</sup>Department of Physics and Astronomy, Ghent University, 9000 Gent, Belgium

<sup>m</sup>II. Physikalisches Institut, Justus-Liebig-Universität Gießen, 35392 Gießen, Germany

<sup>n</sup>SUPA, School of Physics and Astronomy, University of Glasgow, Glasgow G12 8QQ, United Kingdom

<sup>o</sup>Department of Physics, University of Illinois, Urbana, Illinois 61801-3080, USA

<sup>p</sup>Randall Laboratory of Physics, University of Michigan, Ann Arbor, Michigan 48109-1040, USA

<sup>q</sup>Lebedev Physical Institute, 117924 Moscow, Russia

<sup>r</sup>National Institute for Subatomic Physics (Nikhef), 1009 DB Amsterdam, The Netherlands

<sup>s</sup>K.P. Konstantinov Petersburg Nuclear Physics Institute, Gatchina, 188300 Leningrad Region, Russia

<sup>t</sup>Institute for High Energy Physics, Protvino, 142281 Moscow Region, Russia

<sup>u</sup>Institut für Theoretische Physik, Universität Regensburg, 93040 Regensburg, Germany

<sup>v</sup>Istituto Nazionale di Fisica Nucleare, Sezione di Roma, Gruppo Collegato Sanità and Istituto Superiore di Sanità, 00161 Roma, Italy

<sup>w</sup>TRIUMF, Vancouver, British Columbia V6T 2A3, Canada

<sup>x</sup>Department of Physics, Tokyo Institute of Technology, Tokyo 152, Japan

<sup>y</sup>Department of Physics and Astronomy, VU University, 1081 HV Amsterdam, The Netherlands

<sup>z</sup>National Centre for Nuclear Research, 00-689 Warsaw, Poland

<sup>aa</sup>Yerevan Physics Institute, 375036 Yerevan, Armenia

<sup>1</sup>Now at: Brookhaven National Laboratory, Upton, New York 11772-5000, USA

---

## Abstract

Single-spin asymmetries were investigated in inclusive electroproduction of charged pions and kaons from transversely polarized protons at the HERMES experiment. The asymmetries were studied as a function of the azimuthal angle  $\psi$  about the beam direction between the target-spin direction and the hadron production plane, the transverse hadron momentum  $P_T$  relative to the direction of the incident beam, and the Feynman variable  $x_F$ . The  $\sin\psi$  amplitudes are positive for  $\pi^+$  and  $K^+$ , slightly negative for  $\pi^-$  and consistent with zero for  $K^-$ , with particular  $P_T$  but weak  $x_F$  dependences. Especially large asymmetries are observed for two small subsamples of events, where also the scattered electron was recorded by the spectrometer.

*Keywords:*

*PACS:* 13.60.-r, 13.88.+e, 14.20.Dh, 14.65.-q

---

Transverse single-spin asymmetries (SSAs) observed in the azimuthal distributions of hadrons produced in high-energy electromagnetic and hadronic reactions (where either the projectile or the target nucleon is polarized transversely to the beam direction) are a window for our understanding of the nucleon structure and the process of hadronization in the framework of quantum-chromodynamics (QCD). They originate from correlations of the transverse spin of the nucleon and/or the transverse spins of the quarks with transverse quark momentum and could in models be related to spin-orbit effects and to the elusive orbital motion of partons within the nucleon. Left-right cross-section asymmetries  $A_N$  for the inclusive production of various hadrons in hadron-nucleon collisions have been measured over the past three decades by numerous experiments [1–25] for center-of-mass energies in the range 4.9 - 500 GeV. Large values of  $A_N$  were observed for single hadrons in  $p^\uparrow p \rightarrow hX$  reactions at large transverse hadron momenta,  $P_T$ , and large positive values of  $x_F$ , exceeding  $|A_N| = 0.4$  for charged pions. The Feynman variable  $x_F$  is defined as the ratio of the longitudinal hadron momentum  $P_L$  along the beam direction to its maximum possible value. Transverse single-spin asymmetries have also been investigated in semi-inclusive deep-inelastic lepton scattering,  $lN^\uparrow \rightarrow l'hX$ , from transversely polarized hydrogen [26–31], deuterium [32–34], and  $^3\text{He}$  [35] targets. Here, substantial azimuthal SSAs up to about 0.1 have been observed for hydrogen targets. A review of experimental results can be found in Refs. [36] and [37], together with an extended discussion on contemporary theoretical work.

The large size of these single-spin asymmetries indicates the importance of effects beyond the standard leading-twist framework based on collinear factorization. One approach [38] is based on the use of parton distribution and fragmentation functions that are unin-

tegrated in transverse momenta. In this approach, the asymmetries are caused mainly by two mechanisms: the Sivers [39] and Collins [40] effects. The former is related to the transverse-momentum-dependent naive-time-reversal odd Sivers distribution function of unpolarized quarks with non-zero transverse momenta in a transversely polarized nucleon. The latter is related to the chiral-odd transversity distribution of transversely polarized quarks in a transversely polarized nucleon, in conjunction with the transverse-momentum-dependent chiral-odd Collins fragmentation function. The other approach [41–46] links collinear parton dynamics to higher-twist multiparton correlations. Again, two mechanisms dominate where either a twist-three chiral-odd fragmentation function couples to the transversity distribution, or where a twist-three chiral-even distribution function enters with the ordinary leading-twist unpolarized fragmentation function. These approaches have different kinematic domains of validity, but with a region in common. In the past it was believed that they succeeded in reproducing the existing measurements of  $A_N$  in hadron-hadron reactions to a very large extent, and have been shown to be related to and consistent with each other in the kinematic region where they both apply [47]. Recently, however, a sign error was identified [48] that invalidates the good agreement observed earlier. Presently the situation is unsettled [49].

There exist several theoretical expectations for aspects of the SSAs in hadron electroproduction. Their validity depends on the relative magnitude of the three relevant scales  $\Lambda_{\text{QCD}}$ ,  $P_T$  and  $Q$ , where  $\Lambda_{\text{QCD}} \cong 0.3$  GeV is the QCD scale parameter and  $-Q^2$  is the squared four-momentum of the virtual photon that mediates the lepton-nucleon scattering process:

i) Theory makes no reliable prediction for the kinematic region where both  $P_T$  and  $Q$  are small and of order  $\Lambda_{\text{QCD}}$ ;

ii) The twist-three approach leads to a characteristic power suppression by  $1/P_T$  for large  $P_T$ , provided  $P_T$  is the largest scale in the process. For  $P_T < 1$  GeV such power suppressions typically become less efficient;

iii) The Siverts and Collins effects become significant when  $Q^2 > P_T^2$  and  $Q^2 \gg \Lambda_{\text{QCD}}^2$  and give a contribution that is not  $P_T$ -suppressed. For large  $Q^2$ , the dominant contribution to the asymmetry should therefore come from the Siverts and Collins mechanisms. The SSAs measured in semi-inclusive DIS were, in fact, the basis for an extraction of the Siverts and transversity distribution functions and the Collins fragmentation function (see e.g., Refs. [50, 51]);

iv) It was shown that, for the kinematic regime  $Q \gg P_T \gg \Lambda_{\text{QCD}}$ , the descriptions in terms of the Siverts distribution function and of twist-three quark-gluon correlation functions become equivalent [52] and that there also exists a kinematic region in which a twist-three fragmentation function and the leading-twist Collins fragmentation function can be mapped onto one another [53]. For  $P_T^2 \sim Q^2$  one cannot make any quantitative theoretical statement about their connection.

A substantial number of theoretical predictions (see, e.g., Refs. [44, 47, 54–60]) have not yet been confronted with experimental data. More data are required in a wider kinematic range that covers transverse momenta as high as possible but also approaches  $P_T$  values as small as  $\Lambda_{\text{QCD}}$  for both  $A_N$  in hadron-hadron reactions and SSAs in electroproduction of hadrons,  $lp^\uparrow \rightarrow hX$ . This Letter reports on the first measurement of azimuthal SSAs in inclusive electroproduction of charged pions and kaons off transversely polarized protons. It addresses a portion of this unexplored kinematic space.

The data reported here were collected during the period 2002 - 2005 with the HERMES spectrometer [61] using the 27.6 GeV lepton beam (electrons or positrons) incident upon a transversely nuclear-polarized gaseous hydrogen target internal to the HERA lepton storage ring at DESY. The integrated luminosity of the data sample was approximately  $146 \text{ pb}^{-1}$ . The average magnitude of the proton-polarization component perpendicular to the beam direction,  $S_T$ , was  $0.713 \pm 0.063$ . The direction of the target-spin vector was reversed between the “upward” and “downward” directions at 1-3 minute intervals to minimize systematic effects, while both the nuclear polarization and the atomic fraction inside the target cell were measured continuously [62]. The beam was longitudinally polarized and its helicity reversed every few months. A helicity-balanced data sample was used to obtain an effectively unpolarized beam.

Selected events had to contain at least one charged-

hadron track, identified as either a pion or a kaon, within the angular acceptance of the spectrometer ( $\pm 170$  mrad horizontally and  $\pm(40 - 140)$  mrad vertically) independent of whether there was also a scattered lepton in the acceptance or not. Hadrons were distinguished from leptons by using a transition-radiation detector, a scintillator pre-shower counter, and an electromagnetic calorimeter. This resulted in a tiny lepton contamination in the hadron sample of less than 0.1%. Hadrons within the momentum range 2 – 15 GeV were further identified using a dual-radiator ring-imaging Cherenkov detector [63]. This identification is based on a direct ray tracing algorithm that deduces the most probable particle types from the event-level hit pattern of Cherenkov photons on the photomultiplier matrix [64].

The trigger of the experiment was formed, for each detector half, by a coincidence of signals from a scintillation counter in front of the spectrometer magnet and from a scintillator hodoscope and the pre-shower counter behind the magnet, spaced by 1 m, with the requirement of an energy deposit greater than 1.4 GeV in the electromagnetic calorimeter. The trigger was almost 100% efficient for leptons with energies above threshold. The energy threshold of the calorimeter was low enough to trigger also on events with only charged hadrons and no leptons in its geometrical acceptance. In this case, the trigger efficiency was substantially smaller and depended on the hadron momentum  $P_h$ , as well as on the impact position and angle of the hadron track on the calorimeter surface and the hadron multiplicity in the event. Averaged over the hadron multiplicity, the trigger efficiency was about 40 – 45% for hadron momenta greater than approximately 7 GeV and decreased smoothly with decreasing  $P_h$  to about 15% at  $P_h \approx 2$  GeV. In order not to bias the inclusive-hadron sample towards events with a coincident lepton in the detector acceptance, trigger-efficiency corrections dependent on the event topology (e.g., additional lepton or further hadrons in the event) were applied. In total, about  $60 \cdot 10^6$  ( $50 \cdot 10^6$ ) tracks of positively (negatively) charged pions and  $5.1 \cdot 10^6$  ( $2.8 \cdot 10^6$ ) tracks of positively (negatively) charged kaons were collected. These correspond to about  $172 \cdot 10^6$  ( $142 \cdot 10^6$ ) positively (negatively) charged pions and  $14.5 \cdot 10^6$  ( $7.3 \cdot 10^6$ ) positively (negatively) charged kaons after trigger-efficiency correction (cf. Tab. 1), which are used in all of the subsequent results.

As the scattered lepton was not required for the primary analysis, the following hadron variables were used:  $P_T$ , the transverse momentum of the hadron with respect to the lepton beam direction;  $x_F$ , here calculated in the lepton-nucleon center-of-momentum frame;

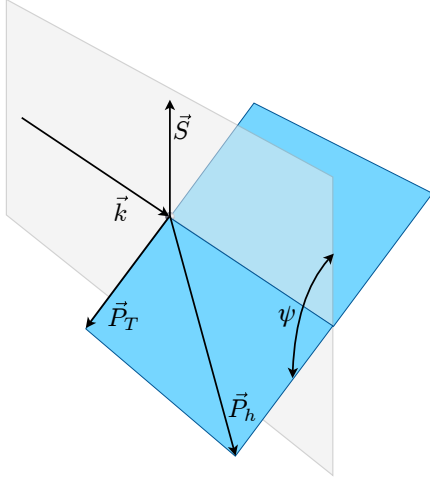


Figure 1: The definition of the azimuthal angle  $\psi$ .

and  $\psi$ , the azimuthal angle about the beam direction between the “upward” target spin direction and the hadron production plane, in accordance with the *Trento Conventions* [65] (see Fig. 1).

The cross section for inclusive electroproduction of hadrons using an unpolarized lepton beam and a transversely polarized target includes a polarization-averaged and a polarization-dependent part and is given for each hadron species as

$$d\sigma = d\sigma_{UU} \left[ 1 + S_T A_{UT}^{\sin\psi} \sin\psi \right]. \quad (1)$$

Here, the first subscript U denotes unpolarized beam, the second subscript U (T) an unpolarized (transversely polarized) target. The dependences of the cross section and of the azimuthal amplitude  $A_{UT}^{\sin\psi}$  on  $P_T$  and  $x_F$  have been omitted. The  $\sin\psi$  azimuthal dependence follows directly from the term  $\vec{S} \cdot (\vec{P}_h \times \vec{k})$  in the spin-dependent part of the cross section (see, e.g., Ref. [60]), with  $\vec{S}$  being the target-spin vector, and  $\vec{k}$  and  $\vec{P}_h$  the three-momenta of the incident lepton and of the final-state hadron, respectively.

The  $\sin\psi$  amplitude  $A_{UT}^{\sin\psi}$  is related to the left-right asymmetry  $A_N$  along the direction of the incident lepton beam and with respect to the nucleon-spin direction,<sup>2</sup> measured with a detector with full  $2\pi$ -coverage in  $\psi$  and constant efficiency, by

$$A_N \equiv \frac{\int_{-\pi}^{2\pi} d\psi d\sigma - \int_0^{\pi} d\psi d\sigma}{\int_{-\pi}^{2\pi} d\psi d\sigma + \int_0^{\pi} d\psi d\sigma} = -\frac{2}{\pi} A_{UT}^{\sin\psi}. \quad (2)$$

<sup>2</sup>The sign convention of  $A_N$  in hadron collisions commonly differs through defining “left” and “right” with respect to the momentum and transverse-spin directions of the incoming polarized hadron.

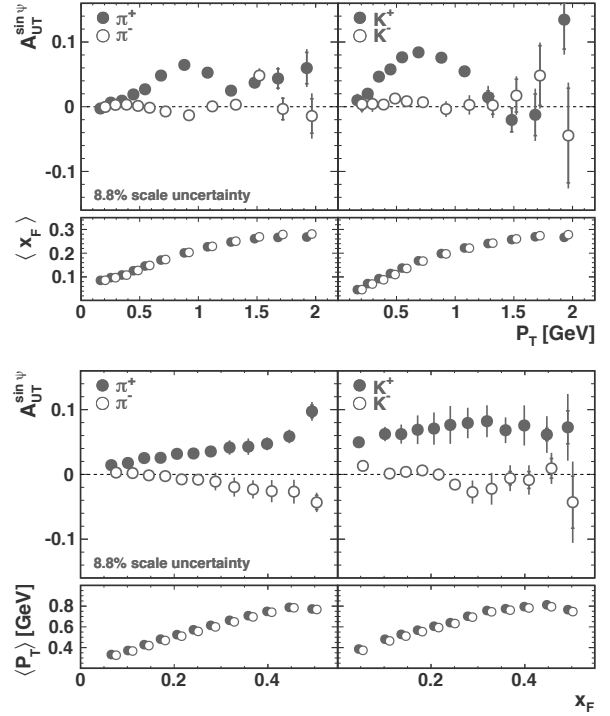


Figure 2:  $A_{UT}^{\sin\psi}$  amplitudes for charged pions and kaons as a function of  $P_T$  (top) and  $x_F$  (bottom). Positive (negative) particles are denoted by closed (open) symbols. When visible, the inner error bars show the statistical uncertainties, while the total ones represent the quadratic sum of statistical and systematic uncertainties. Not shown is an additional 8.8% scale uncertainty due to the precision of the measurement of the target polarization. The bottom subpanels show the  $P_T$  dependence ( $x_F$  dependence) of the average  $x_F$  ( $P_T$ ). Data points for negative particles are slightly shifted horizontally for legibility.

Experimentally, the  $A_{UT}^{\sin\psi}$  amplitudes were extracted by performing a maximum-likelihood fit to the cross section of Eq. 1, i.e., the measured yield distribution for the two target-spin states weighted with the inverse of the trigger efficiencies and luminosity, binned in  $P_T$  and  $x_F$ , but unbinned in  $\psi$ . The detection efficiency, if independent of the target-spin state, cancels in the fit as long as the polarization-weighted luminosity vanishes, i.e.,  $\int S_T(t)L(t)dt = 0$ , as is the case for the present data.

The extracted  $A_{UT}^{\sin\psi}$  amplitudes for charged pions and kaons are presented as a function of  $P_T$  in the top panels of Fig. 2. The amplitudes are positive for the positive hadrons, being slightly larger for kaons compared to pions. They rise smoothly with  $P_T$  up to a maximum value of approximately 0.06 (0.08) for pions (kaons) at  $P_T \simeq 0.8$  GeV and then decrease again with increasing  $P_T$ . Note that at  $P_T = 0$  GeV the amplitude  $A_{UT}^{\sin\psi}$  vanishes by definition. For  $P_T > 1.3$  GeV, the statistical un-

certainties increase substantially with  $P_T$ . Here, there is an indication of an increase of the amplitude for pions, while for kaons it is compatible with zero within the uncertainties, apart from the point at the highest  $P_T$ , where the amplitude is 2.8 standard deviations above zero. For negative hadrons the amplitudes are much smaller in magnitude, sometimes positive and sometimes negative, apart from the  $\pi^-$  point at  $P_T = 1.5$  GeV. Detailed investigations of the data and the analysis leading to this exceptionally large asymmetry amplitude have not revealed any instrumental origin.

In the bottom panels of Fig. 2, the measured  $A_{UT}^{\sin\psi}$  amplitudes are presented as a function of  $x_F$ . For positive pions, the amplitudes are positive everywhere and increase nearly linearly with  $x_F$  up to a value of approximately 0.06, with the exception of the point in the highest  $x_F$  bin, where the value is  $0.10 \pm 0.01_{\text{stat}} \pm 0.01_{\text{sys}}$ . For negative pions, the amplitude is negative over most of the  $x_F$  range and decreases linearly down to a value of about -0.04 for the last  $x_F$  bin. These  $x_F$  dependences of the pion asymmetry amplitudes look similar to the one observed in hadron-hadron collisions. For positive kaons, the amplitude is about constant around 0.07, with some small variation with  $x_F$ . For negative kaons, the asymmetry amplitude is compatible with zero over most of the  $x_F$  range, with a small positive excursion in the lowest  $x_F$  bin, and a negative one in the region around  $x_F = 0.3$ .

The variables  $x_F$  and  $P_T$  are strongly correlated in these measurements as can be seen from the bottom sub-panels of Fig. 2, where they are shown at the average bin kinematics. Hence, any observed kinematic dependence of  $A_{UT}^{\sin\psi}$  cannot be uniquely ascribed to the variable plotted against but may stem from the underlying dependence on the kinematic variable over which the data are integrated. For this reason, a two-dimensional extraction of the asymmetry amplitudes was performed by binning simultaneously in  $P_T$  and  $x_F$ . The resulting  $A_{UT}^{\sin\psi}$  amplitudes are shown as a function of  $P_T$  in four slices of  $x_F$  in Fig. 3, and in Fig. 4 as a function of  $x_F$  in four slices of  $P_T$ . Only data points with a statistical uncertainty of the asymmetry amplitude smaller than 0.1 are shown. The  $P_T$  dependence in the four  $x_F$  slices is very similar in shape and magnitude, apart from increased statistical fluctuations. For positive pions the amplitude is seen to be essentially independent of  $x_F$  in all four slices in  $P_T$ . Therefore, it can be concluded that the apparent increase of the magnitude of the asymmetry amplitude with  $x_F$  seen for positive pions in Figure 2 is just a reflection of the underlying dependence on  $P_T$ . In contrast, for negative pions the decrease with  $x_F$  follows the one observed in the one-dimensional extrac-

tion. The dependence on  $x_F$  of the kaon asymmetry amplitudes is less pronounced in the two-dimensional extraction, with a slight tendency towards an increase (decrease) with  $x_F$  for positive (negative) kaons. Note that in measurements of inclusive SSAs in proton-proton collisions,  $A_N$  is seen to rise strongly for values of  $x_F$  larger than about 0.3-0.4. For charged pions [22] and neutral pions [23] such an increase of  $A_N$  with  $x_F$  was seen even after binning the data in slices of  $P_T$ .

In Figs. 2–5, the systematic uncertainties are added in quadrature to the statistical ones. One contribution arises from different methods employed for the trigger-efficiency correction. An additional contribution, added in quadrature to the previous one, arises from typical effects due to non-perfect experimental resolution and acceptance, and is determined in a manner to include the effects of the necessary binning of finite statistics. This second contribution was determined from a high-statistics Monte Carlo data sample obtained from a simulation using the program PYTHIA 6.2 [66, 67]. This simulation [68] contained a full description of the detector, including effects such as acceptance, correction for particle deflection in the vertical target holding field, losses due to decay in flight and secondary strong interactions, and particle identification. In addition, a spin-dependent azimuthal asymmetry was imposed on the simulated event sample according to Eq. (1). The functional form  $\mathcal{A}_{UT,MC}^{\sin\psi}$  is a Taylor expansion in  $P_T$  (up to fifth order) and  $x_F$  (up to first order) around the average kinematics of the entire experimental data sample. The set of (up to) twelve parameters for each hadron species was obtained in a maximum-likelihood fit to the experimental data where the number of terms in the expansion was tuned to describe all measured asymmetry amplitudes. The  $\sin\psi$  amplitudes  $A_{UT,MC}^{\sin\psi}$  were then extracted from the now spin-dependent Monte Carlo sample in the same way as described above for data. The total systematic uncertainty in each bin corresponds to the maximum value of either the (in most bins negligibly small) statistical uncertainty in the Monte Carlo sample or the deviation between the model function  $\mathcal{A}_{UT,MC}^{\sin\psi}$  evaluated at the average kinematics of the bin and the reconstructed  $A_{UT,MC}^{\sin\psi}$  amplitude. This calculational approach is designed to address, among others, the differences between the asymmetry amplitudes evaluated at the average values of their kinematical dependences and the asymmetry amplitudes averaged over the bin range(s) of the kinematical dependences. These differences can become large whenever an amplitude's dependence deviates significantly from linear behavior over the width of the bin in that dependence. This makes the one-dimensional representation of Fig. 2, where one inte-

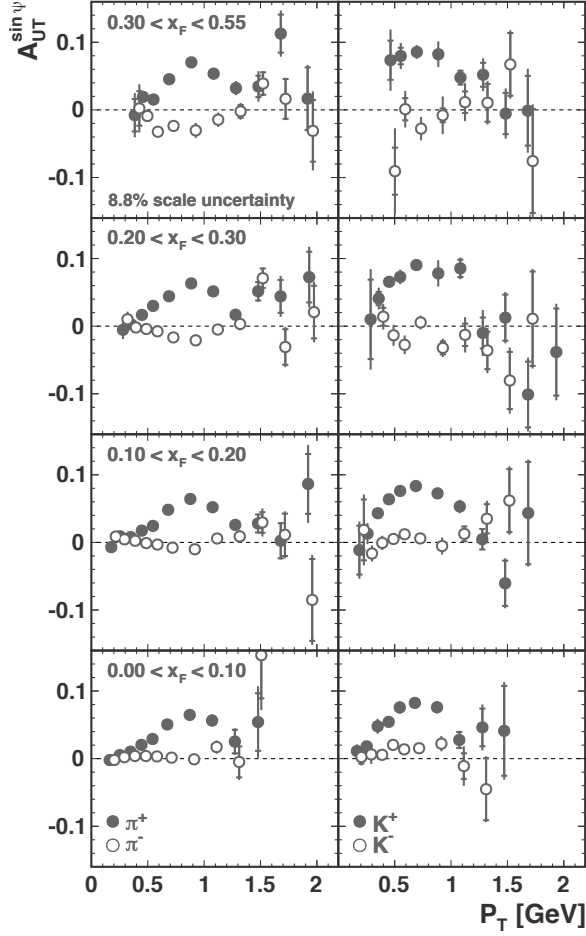


Figure 3:  $A_{UT}^{\sin\psi}$  amplitudes for charged pions and kaons as a function of  $P_T$  for various slices in  $x_F$ . Symbol definitions and additional 8.8% scale uncertainty as in Fig. 2.

grates over the whole range in the variable not shown, more susceptible to systematic deviations. These can be observed, e.g., in the  $x_F$  dependence of the  $K^+$  asymmetry amplitudes, where the integration is over a strongly varying  $P_T$  dependence. Additionally, the uncertainty on the measurement of the target polarization produces a 8.8% scale uncertainty on the value of  $A_{UT}^{\sin\psi}$  that is not included in the error bars/bands. Other possible sources of systematic uncertainty not included in the Monte Carlo simulation such as time-dependence of the measured amplitudes and the effect of different beam charges were found to be negligible.

The inclusive data set presumably is a mixture of various contributions with different kinematic dependences. Therefore, it is difficult to draw conclusions about the underlying physics from the observed kinematic depen-

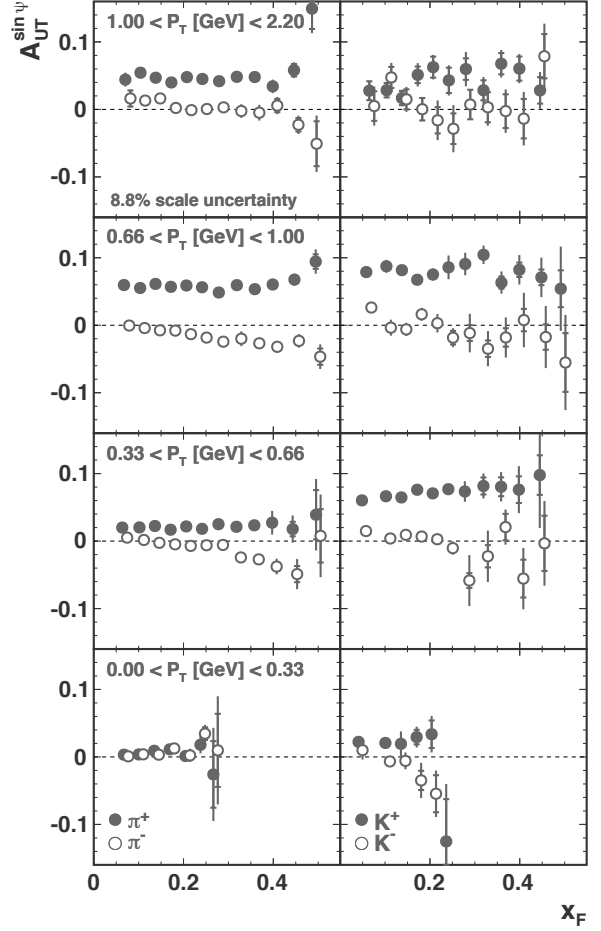


Figure 4:  $A_{UT}^{\sin\psi}$  amplitudes for charged pions and kaons as a function of  $x_F$  for various slices in  $P_T$ . Symbol definitions and additional 8.8% scale uncertainty as in Fig. 2.

dences of the inclusive asymmetry amplitudes. More insight may be gained by studying separately the asymmetries for the events without a scattered lepton in the acceptance ('anti-tagged' category) and the events with a scattered lepton in the acceptance ('tagged' or semi-inclusive category). These categories cover different kinematic regimes and are defined as follows:

1) 'Anti-tagged' category: The undetected lepton in most cases had a small scattering angle and remained within the beam pipe. Hence  $Q^2$  is small and  $P_T$  is the only hard scale. For these events, the difference between the transverse hadron momentum with respect to the beam direction,  $P_T$ , and with respect to the virtual-photon direction,  $P_{h\perp}$ , is small. The latter was used in the previous analyses of SSAs in semi-inclusive deep-inelastic scattering [26–28]. The present data sample

subsample	$\pi^+$	$\pi^-$	$K^+$	$K^-$
'anti-tagged'	170.5	140.7	14.3	7.2
'tagged'	1.93	1.49	0.26	0.13
DIS, $0.2 < z < 0.7$	0.69	0.49	0.12	0.05
DIS, $z > 0.7$	0.061	0.037	0.013	0.001

Table 1: Accumulated yields of hadrons (in million) for the various event samples without and with an electron in the spectrometer acceptance, after correction for trigger efficiency. The DIS subsamples are part of the 'tagged' category, as explained in the text.

is dominated by the kinematic regime  $Q^2 \approx 0$  GeV<sup>2</sup> of quasireal photoproduction where the cross section is largest and where the hadronic component of the photon plays an important role. Generally speaking, in this kinematic range  $l + p^\uparrow$  reactions are expected to be quite similar in nature to  $h + p^\uparrow$  reactions. The 'anti-tagged' category contains a small contamination of events at higher  $Q^2$  where the electron is scattered into the horizontal gap of the spectrometer. These events amount to about one third in statistics of the semi-inclusive category, discussed below. Another tiny high- $Q^2$  contamination arises from lepton scattering angles beyond the maximum polar angular acceptance of the spectrometer. These events occur dominantly at high  $P_T$ . Here, the large angle of the virtual photon with respect to the beam axis often results in a significantly larger  $P_T$  than  $P_{h,\perp}$  of the hadrons. After correction for trigger efficiency, about 98% of all hadrons belong to the 'anti-tagged' category. The fraction of these hadrons with respect to the total inclusive sample is nearly 100% at low  $P_T$ . It decreases monotonically to about 85 – 90% for positive hadrons and to more than 90% for negative hadrons at the highest  $P_T$  values.

2) 'Tagged' or semi-inclusive category: The scattered positron was recorded in the spectrometer acceptance and kinematic quantities like  $y$ ,  $z$ ,  $Q^2$ ,  $x$ , and  $W^2$  could be determined, where in the laboratory system  $y \equiv P \cdot q / (P \cdot k)$  is the fractional beam energy carried by the virtual photon and  $z \equiv P \cdot P_h / (P \cdot q)$  is the fractional virtual-photon energy carried by the hadron. The quantity  $x \equiv Q^2 / (2P \cdot q)$  is the Bjorken scaling variable with  $-Q^2 = q^2 \equiv (k - k')^2$ , and  $W^2 \equiv (P + q)^2$  is the squared invariant mass of the virtual-photon nucleon system. Here,  $P$ ,  $k$ ,  $k'$ , and  $P_h$  are the four-momenta of the target nucleon, the incident and scattered lepton, and the produced hadron, respectively. This category can be further divided into several subsamples covering different kinematic regions.

For the present analysis, two of these subsamples have been selected that affect substantially the observed

asymmetries at large  $P_T$ :

- *DIS events with  $0.2 < z < 0.7$* : This subsample is identical to the one used previously [26–28] for the determination of azimuthal transverse single-spin asymmetries in semi-inclusive deep-inelastic scattering related to the Sivers and transversity distributions and the Collins fragmentation function. Here, events were selected according to the kinematic requirements  $Q^2 > 1$  GeV<sup>2</sup>,  $W^2 > 10$  GeV<sup>2</sup>,  $0.023 < x < 0.4$ , and  $0.1 < y < 0.95$ . The fractional hadron energy was required to be in the range  $0.2 < z < 0.7$ . For this sample,  $\langle Q^2 \rangle$  rises from  $\sim 2.2$  GeV<sup>2</sup> at low  $P_T$  to  $\sim 4.3$  GeV<sup>2</sup> at high  $P_T$ , and  $\langle Q^2 \rangle$  is always larger than  $\langle P_T^2 \rangle$  apart from the two highest  $P_T$  bins;

- *DIS events with  $z > 0.7$* : The kinematic requirements are identical to those of the above subsample, apart from the requirement for the fractional hadron energy. Only hadrons with  $z > 0.7$  are selected. The average value of  $Q^2$  rises from  $\sim 1.5$  GeV<sup>2</sup> to  $\sim 5.5$  GeV<sup>2</sup> and  $\langle Q^2 \rangle > \langle P_T^2 \rangle$  over the whole  $P_T$  range.

The total number of hadron tracks in the 'anti-tagged' and the 'tagged' categories and in the two DIS subsamples is listed in Table 1. The remaining events of the 'tagged' category contribute only at  $x_F < 0.2$  and  $P_T < 0.9$  GeV and will not be discussed further.

In Figure 5, the  $A_{UT}^{\sin\psi}$  amplitudes are presented as a function of  $P_T$  for the 'anti-tagged' category and the two DIS subsamples with  $0.2 < z < 0.7$  and  $z > 0.7$ , respectively. Also shown are the relative fractions of these two subsamples with respect to the total inclusive sample of the corresponding hadron species after correction for trigger efficiency. The relative fractions are generally larger for positive hadrons than for negative hadrons. For  $P_T < 1$  GeV, the fractions are below 1%. In the highest two  $P_T$  bins, the fraction of DIS events with  $z > 0.7$  dominates for positive hadrons and reaches values of about 6%, while the DIS contribution with  $0.2 < z < 0.7$  stays below 4%. As can be seen from Figure 5, the asymmetry amplitudes for the 'anti-tagged' category and for the two subsamples of the 'tagged' category show several remarkable peculiarities:

- *'Anti-tagged' category*: The asymmetry amplitudes are, over most of the  $P_T$  range, essentially identical to the inclusive amplitudes as expected from the fact that this sample comprises about 98% of the whole statistics. One can therefore safely conclude that essentially all of the kinematic dependences of the inclusive data set observed for  $P_T$  below approximately 1.5 GeV originate from quasi-real photoproduction. Since  $P_T$  is the only hard scale, the origin of the asymmetries can most likely be explained by higher-twist contributions. At low values of  $P_T$ , where one observes a rise of the asym-

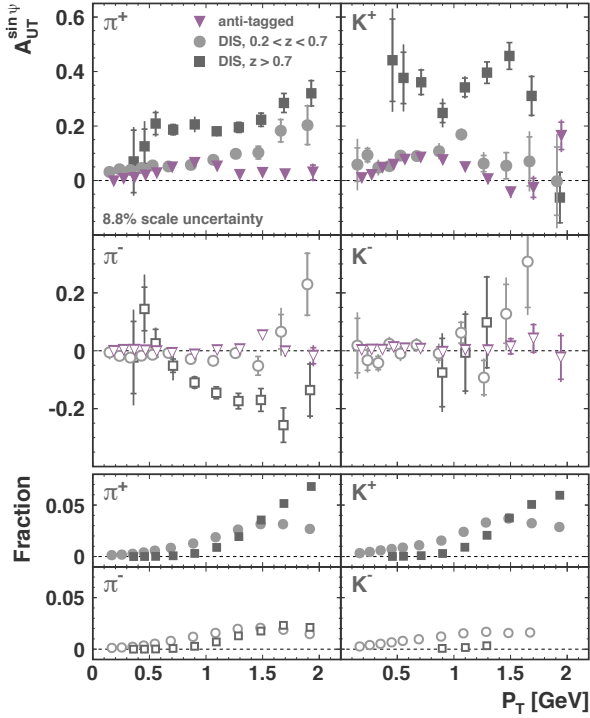


Figure 5:  $A_{UT}^{\sin\psi}$  amplitudes for charged pions and kaons for the ‘anti-tagged’ category and the two DIS subsamples with  $0.2 < z < 0.7$  and  $z > 0.7$ , respectively. Also shown are the relative fractions of the two DIS subsamples with respect to the total inclusive sample of the corresponding hadron species after correction for trigger efficiency. Positive (negative) particles are denoted by filled (open) symbols. Inner error bars show the statistical uncertainties and the total error bars represent statistical and systematic uncertainties added in quadrature. Not shown is an additional 8.8% scale uncertainty due to the precision of the measurement of the target polarization.

metry amplitudes for positive hadrons,  $P_T$  is comparable to  $\Lambda_{\text{QCD}}$  and theory cannot presently make reliable predictions about the magnitude and  $P_T$  dependence of the amplitudes. At high  $P_T$ , the ‘anti-tagged’ asymmetry amplitude is consistently smaller than the inclusive amplitude for positive pions and its  $P_T$  dependence is, within uncertainties, compatible with a constant or a decrease with  $P_T$  as one would expect for this class of events [59, 60]. At  $P_T > 1.3$  GeV the contributions from the other subsamples become sizable causing the increase with  $P_T$  observed for the inclusive asymmetry amplitude.

- *DIS events with  $0.2 < z < 0.7$* : For positive pions,  $A_{UT}^{\sin\psi}$  is positive and larger than the ‘anti-tagged’ amplitude. It rises rather linearly with  $P_T$  from a value of approximately 0.04 at low  $P_T$  to approximately 0.2 at the highest  $P_T$  values, where the statistical uncertainties are

rather large. For negative pions, the amplitude is (apart from the two highest  $P_T$  points) consistently negative and larger in magnitude than the asymmetry amplitude for the ‘anti-tagged’ sample over the whole range of  $P_T$ . As stated above,  $Q^2$  is the largest scale over essentially the whole  $P_T$  range and transverse-momentum-dependent distribution and fragmentation functions can contribute without  $P_T$ -suppression. Since the angle  $\psi$  and the Sivers angle  $\phi - \phi_s$  are closely related, one can expect that the observed  $P_T$  dependence is predominantly caused by the Sivers effect. In fact, the asymmetries are very similar to those in Ref. [27], where it was concluded that the small amplitudes for  $\pi^-$  require cancellation effects, e.g., from a down-quark Sivers function opposite in sign to the dominant up-quark Sivers function.

- *DIS events with  $z > 0.7$* : Large asymmetries are observed for this subsample for both pion charges and especially for positive kaons, where the amplitudes reach values of more than 0.4. For positive pions the amplitude is rather constant with a value of around 0.2 in the  $P_T$  range 0.5–1.5 GeV, and rises up to a value above 0.3 at the highest  $P_T$  bin. For negative pions, the amplitude is negative and decreases from approximately zero at  $P_T \sim 0.5$  GeV down to a value of about -0.2 at high  $P_T$ . This subsample receives contributions from processes that can become significant only in this kinematic region. Pions receive contributions from decays of exclusive mesons like, e.g., the  $\rho$  meson [69] that can contribute up to about 50% (30%) to the yield of  $\pi^-$  ( $\pi^+$ ) at large  $z$  [70]. For kaons, the corresponding contributions from  $\phi$  decays are less than 10%. For positive pions there is in addition a contribution from exclusive production,  $lp \rightarrow l'\pi^+n$ , which has, however, been measured [71] to constitute only approximately 3% of this sample. The corresponding contributions for the quasi-exclusive production of negative pions from  $lp \rightarrow l'\pi^-\Delta^{++}$  or positive kaons from  $lp \rightarrow l'K^+\Lambda$  are expected to be even smaller [72] and no such quasi-exclusive channel exists for negative kaons. The large asymmetry amplitude seen for negative pions may indicate that a large fraction of events in this subsample stems from the favoured fragmentation of the struck quark (here the down quark) and that the asymmetry possibly preserves information from the down-quark Sivers function without dilution from disfavoured fragmentation of the otherwise dominating up quark. Indeed, the signs and relative magnitudes of the pion and kaon asymmetry amplitudes observed are not inconsistent with the values of the up and down quark Sivers functions extracted in phenomenological fits [50].

In summary, transverse azimuthal single-spin asym-



metries are measured in inclusive and semi-inclusive electroproduction of charged pions and kaons. A two-dimensional extraction of the asymmetry amplitudes is performed by binning simultaneously in the component of the hadron-momentum transverse to the incoming lepton beam,  $P_T$ , and the Feynman- $x$  variable,  $x_F$ . For positive pions, the resulting amplitudes are found to be essentially independent of  $x_F$ . The apparent increase with  $x_F$  after integration over  $P_T$  is mostly a reflection of the underlying dependence on  $P_T$ . For negative pions, and less significantly for negative (positive) kaons, the asymmetry amplitudes decrease (increase) with  $x_F$ , also in the case of a two-dimensional extraction. The amplitudes as a function of  $P_T$  are positive for the positive hadrons and slightly larger for  $K^+$  compared to  $\pi^+$ . They rise smoothly with  $P_T$  from zero at low  $P_T$  up to a maximum value of approximately 0.06 (0.08) for pions (kaons) at  $P_T \simeq 0.8$  GeV and then decrease with increasing  $P_T$ . The data sample is dominated by the kinematic regime  $Q^2 \approx 0$  GeV<sup>2</sup> of quasi-real photo-production, where  $P_T$  is the only hard scale. The origin of the observed asymmetries can, therefore, most likely be explained by higher-twist contributions. At  $P_T$  values above 1.5 GeV there are sizable contributions from events with an electron in the acceptance and large values of  $Q^2$ . The asymmetries for the subsample within DIS kinematics and fractional energies of the hadron in the range  $0.2 < z < 0.7$  can likely be related to the transverse-momentum dependent Sivvers distribution function. Very large asymmetry amplitudes are observed for positive pions and kaons and negative pions for the DIS subsample with high values of the fractional hadron energy  $z$ . In this kinematic regime exclusive processes can contribute substantially to the asymmetry and effects from the favoured fragmentation of the struck quark dominate. The data may be very helpful in formulating a better understanding of spin-orbit effects of partons within the nucleon.

We gratefully acknowledge the DESY management for its support and the staff at DESY and the collaborating institutions for their significant effort. This work was supported by the Ministry of Economy and the Ministry of Education and Science of Armenia; the FWO-Flanders and IWT, Belgium; the Natural Sciences and Engineering Research Council of Canada; the National Natural Science Foundation of China; the Alexander von Humboldt Stiftung, the German Bundesministerium für Bildung und Forschung (BMBF), and the Deutsche Forschungsgemeinschaft (DFG); the Italian Istituto Nazionale di Fisica Nucleare (INFN); the MEXT, JSPS, and G-COE of Japan; the Dutch Foundation for Fundamenteel Onderzoek der Materie

(FOM); the Russian Academy of Science and the Russian Federal Agency for Science and Innovations; the Basque Foundation for Science (IKERBASQUE) and the UPV/EHU under program UFI 11/55; the U.K. Engineering and Physical Sciences Research Council, the Science and Technology Facilities Council, and the Scottish Universities Physics Alliance; the U.S. Department of Energy (DOE) and the National Science Foundation (NSF); as well as the European Community Research Infrastructure Integrating Activity under the FP7 "Study of strongly interacting matter (HadronPhysics3, Grant Agreement number 283286)".

## References

- [1] L. Dick, et al., Phys. Lett. B57 (1975) 93.
- [2] R. Klem, et al., Phys. Rev. Lett. 36 (1976) 929–931.
- [3] W. Dragoset, et al., Phys. Rev. D18 (1978) 3939–3954.
- [4] J. Antille, et al., Phys. Lett. B94 (1980) 523.
- [5] V. Apokin, et al., Phys. Lett. B243 (1990) 461–464.
- [6] D. Adams, et al. (E581/E704 Collaboration), Phys. Lett. B261 (1991) 201–206.
- [7] D. Adams, et al. (E704 Collaboration), Phys. Lett. B264 (1991) 462–466.
- [8] D. Adams, et al. (E581/E704 Collaborations), Z. Phys. C56 (1992) 181–184.
- [9] D. Adams, et al. (E581/E704 Collaborations), Phys. Lett. B276 (1992) 531–535.
- [10] A. Bravar, et al. (E704 Collaboration), Phys. Rev. Lett. 75 (1995) 3073–3077.
- [11] D. Adams, et al. (E704 Collaboration), Phys. Rev. D53 (1996) 4747–4755.
- [12] A. Bravar, et al. (E704 Collaboration), Phys. Rev. Lett. 77 (1996) 2626–2629.
- [13] V. Abramov, et al., Nucl. Phys. B492 (1997) 3–17. [arXiv:hep-ex/0110011](https://arxiv.org/abs/hep-ex/0110011).
- [14] D. Adams, et al. (E704 Collaboration), Nucl. Phys. B510 (1998) 3–11.
- [15] K. Krueger, et al., Phys. Lett. B459 (1999) 412–416.
- [16] C. Allgower, et al., Phys. Rev. D65 (2002) 092008.
- [17] J. Adams, et al. (STAR Collaboration), Phys. Rev. Lett. 92 (2004) 171801. [arXiv:hep-ex/0310058](https://arxiv.org/abs/hep-ex/0310058).
- [18] S. Adler, et al. (PHENIX Collaboration), Phys. Rev. Lett. 95 (2005) 202001. [arXiv:hep-ex/0507073](https://arxiv.org/abs/hep-ex/0507073).
- [19] A. Bazilevsky, et al., Phys. Lett. B650 (2007) 325–330. [arXiv:hep-ex/0610030](https://arxiv.org/abs/hep-ex/0610030).
- [20] M. Togawa (PHENIX Collaboration), AIP Conf. Proc. 915 (2007) 689–692.
- [21] I. Arsene, et al. (BRAHMS Collaboration), Phys. Rev. Lett. 98 (2007) 252001. [arXiv:hep-ex/0701041](https://arxiv.org/abs/hep-ex/0701041).
- [22] I. Arsene, et al. (BRAHMS Collaboration), Phys. Rev. Lett. 101 (2008) 042001. [arXiv:0801.1078](https://arxiv.org/abs/0801.1078) [[nucl-ex](#)].
- [23] B. Abelev, et al. (STAR Collaboration), Phys. Rev. Lett. 101 (2008) 222001. [arXiv:0801.2990](https://arxiv.org/abs/0801.2990) [[hep-ex](#)].
- [24] J. Lee, F. Videbaek (BRAHMS Collaboration) (2009). [arXiv:0908.4551](https://arxiv.org/abs/0908.4551) [[hep-ex](#)].
- [25] A. Adare, et al. (PHENIX Collaboration), Phys. Rev. D82 (2010) 112008. [arXiv:1009.4864](https://arxiv.org/abs/1009.4864) [[hep-ex](#)].
- [26] A. Airapetian, et al. (HERMES Collaboration), Phys. Rev. Lett. 94 (2005) 012002. [arXiv:hep-ex/0408013](https://arxiv.org/abs/hep-ex/0408013).
- [27] A. Airapetian, et al. (HERMES Collaboration), Phys. Rev. Lett. 103 (2009) 152002. [arXiv:0906.3918](https://arxiv.org/abs/0906.3918) [[hep-ex](#)].

- [28] A. Airapetian, et al. (HERMES Collaboration), Phys. Lett. B693 (2010) 11–16. [arXiv:1006.4221 \[hep-ex\]](#).
- [29] M. G. Alekseev, et al. (COMPASS Collaboration), Phys. Lett. B692 (2010) 240–246. [arXiv:arXiv:1005.5609 \[hep-ex\]](#).
- [30] C. Adolph, et al. (COMPASS Collaboration), Phys. Lett. B717 (2012) 376–382. [arXiv:1205.5121 \[hep-ex\]](#).
- [31] C. Adolph, et al. (COMPASS Collaboration), Phys. Lett. B717 (2012) 383–389. [arXiv:1205.5122 \[hep-ex\]](#).
- [32] V. Alexakhin, et al. (COMPASS Collaboration), Phys. Rev. Lett. 94 (2005) 202002. [arXiv:hep-ex/0503002](#).
- [33] E. Ageev, et al. (COMPASS Collaboration), Nucl. Phys. B765 (2007) 31–70. [arXiv:hep-ex/0610068](#).
- [34] M. Alekseev, et al. (COMPASS Collaboration), Phys. Lett. B673 (2009) 127–135. [arXiv:0802.2160 \[hep-ex\]](#).
- [35] X. Qian, et al. (The Jefferson Lab Hall A Collaboration), Phys. Rev. Lett. 107 (2011) 072003. [arXiv:1106.0363 \[nucl-ex\]](#).
- [36] U. D’Alesio, F. Murgia, Prog. Part. Nucl. Phys. 61 (2008) 394–454. [arXiv:0712.4328 \[hep-ph\]](#).
- [37] V. Barone, F. Bradamante, A. Martin, Prog. Part. Nucl. Phys. 65 (2010) 267–333. [arXiv:1011.0909 \[hep-ph\]](#).
- [38] M. Anselmino, M. Boglione, F. Murgia, Phys. Lett. B362 (1995) 164–172. [arXiv:hep-ph/9503290](#).
- [39] D. W. Sivers, Phys. Rev. D41 (1990) 83.
- [40] J. C. Collins, Nucl. Phys. B396 (1993) 161–182. [arXiv:hep-ph/9208213](#).
- [41] J. Qiu, G. F. Sterman, Phys. Rev. D59 (1999) 014004. [arXiv:hep-ph/9806356](#).
- [42] Y. Kanazawa, Y. Koike, Phys. Lett. B478 (2000) 121–126. [arXiv:hep-ph/0001021](#).
- [43] Y. Kanazawa, Y. Koike, Phys. Lett. B490 (2000) 99–105. [arXiv:hep-ph/0007272](#).
- [44] Y. Koike, Nucl. Phys. A721 (2003) 364–367. [arXiv:hep-ph/0211400](#).
- [45] Y. Koike, AIP Conf. Proc. 675 (2003) 449–453. [arXiv:hep-ph/0210396](#).
- [46] C. Kouvaris, et al., Phys. Rev. D74 (2006) 114013. [arXiv:hep-ph/0609238](#).
- [47] Y. Koike, W. Vogelsang, F. Yuan, Phys. Lett. B659 (2008) 878–884. [arXiv:0711.0636 \[hep-ph\]](#).
- [48] Z.-B. Kang, et al., Phys. Rev. D83 (2011) 094001. [arXiv:1103.1591 \[hep-ph\]](#).
- [49] A. Metz, et al., Phys. Rev. D86 (2012) 094039. [arXiv:1209.3138 \[hep-ph\]](#).
- [50] M. Anselmino, et al., J. Phys. Conf. Ser. 295 (2011) 012062. [arXiv:1012.3565 \[hep-ph\]](#).
- [51] M. Anselmino, et al., Nucl. Phys. Proc. Suppl. 191 (2009) 98–107. [arXiv:0812.4366 \[hep-ph\]](#).
- [52] X. Ji, et al., Phys. Lett. B638 (2006) 178–186. [arXiv:hep-ph/0604128](#).
- [53] F. Yuan, J. Zhou, Phys. Rev. Lett. 103 (2009) 052001. [arXiv:0903.4680 \[hep-ph\]](#).
- [54] X. Ji, et al., Phys. Rev. Lett. 97 (2006) 082002. [arXiv:hep-ph/0602239](#).
- [55] H. Eguchi, Y. Koike, K. Tanaka, Nucl. Phys. B752 (2006) 1–17. [arXiv:hep-ph/0604003](#).
- [56] H. Eguchi, Y. Koike, K. Tanaka, Nucl. Phys. B763 (2007) 198–227. [arXiv:hep-ph/0610314](#).
- [57] A. Bacchetta, et al., JHEP 08 (2008) 023. [arXiv:0803.0227 \[hep-ph\]](#).
- [58] H. Beppu, et al., Phys. Rev. D82 (2010) 054005. [arXiv:1007.2034 \[hep-ph\]](#).
- [59] Z.-B. Kang, et al., Phys. Rev. D84 (2011) 034046. [arXiv:1106.3514 \[hep-ph\]](#).
- [60] M. Anselmino, et al., Phys. Rev. D81 (2010) 034007. [arXiv:0911.1744 \[hep-ph\]](#).
- [61] K. Ackerstaff, et al. (HERMES Collaboration), Nucl. Instrum. Meth. A417 (1998) 230–265. [arXiv:hep-ex/9806008](#).
- [62] A. Airapetian, et al. (HERMES Collaboration), Nucl. Instrum. Meth. A540 (2005) 68–101. [arXiv:physics/0408137](#).
- [63] N. Akopov, et al., Nucl. Instrum. Meth. A479 (2002) 511–530. [arXiv:physics/0104033](#).
- [64] A. Airapetian, et al. (HERMES Collaboration), Phys. Rev. D87 (2013) 012010. [arXiv:1204.4161 \[hep-ex\]](#).
- [65] A. Bacchetta, et al., Phys. Rev. D70 (2004) 117504. [arXiv:hep-ph/0410050](#).
- [66] T. Sjöstrand, et al., Comput. Phys. Commun. 135 (2001) 238–259. [arXiv:hep-ph/0010017](#).
- [67] T. Sjöstrand, L. Lonnblad, S. Mrenna (2001). [arXiv:hep-ph/0108264](#).
- [68] A. Airapetian, et al. (HERMES Collaboration), JHEP 08 (2010) 130. [arXiv:1002.3921 \[hep-ex\]](#).
- [69] A. Airapetian, et al. (HERMES Collaboration), Phys. Lett. B679 (2009) 100–105. [arXiv:0906.5160 \[hep-ex\]](#).
- [70] A. Airapetian, et al. (HERMES Collaboration), Phys. Rev. D87 (2013) 074029. [arXiv:1212.5407 \[hep-ex\]](#).
- [71] A. Airapetian, et al. (HERMES Collaboration), Phys. Lett. B682 (2010) 345–350. [arXiv:0907.2596 \[hep-ex\]](#).
- [72] M. Diehl, et al., Phys. Rev. D72 (2005) 034034. [arXiv:hep-ph/0506171](#).